Quark matter in light neutron stars

Márcio Ferreira,[*] Renan Câmara Pereira,[†] and Constança Providência[‡]
CFisUC, Department of Physics, University of Coimbra, P-3004 - 516 Coimbra, Portugal

(Received 20 July 2020; accepted 2 October 2020; published 27 October 2020)

Higher-order repulsive interactions are included in the three-flavor Nambu–Jona-Lasinio model in order to describe the quark phase of an hybrid star. The effect of 4-quark and 8-quark vector-isoscalar interactions in the stability of hybrid star configurations is analyzed. The presence of a 8-quark vector-isoscalar channel is seen to be crucial in generating large quark branches in the $M(R)$ diagram. This is due to its stiffening effect on the quark matter equation of state which arises from the nonlinear density dependence of the speed of sound. This additional interaction channel allows for the appearance of a quark core at moderately low NS masses, $\sim 1\ M_\odot$, and provides the required repulsion to preserve the star stability up to $\sim 2.1\ M_\odot$. Furthermore, we show that both the heaviest NS mass generated, $M_{\rm max}$, and its radius, $R_{\rm max}$, are quite sensitive to the strength of 8-quark vector-isoscalar channel, leading to a considerable decrease of $R_{\rm max}$ as the coupling increases. This behavior imprints a considerable deviation from the purely hadronic matter equation of state in the $\Lambda(M)$ diagram, which might be a possible signature of the quark matter existence, even for moderately low NS masses, $\sim 1.4\ M_\odot$. The resulting $M(R)$ and $\Lambda(R)$ relations are in accordance with the latest astrophysical constraints from NICER and LIGO/Virgo observations, respectively.

DOI: 10.1103/PhysRevD.102.083030

I. INTRODUCTION

Neutron stars (NS) have been the focus of many experimental and theoretical studies in astrophysics, nuclear, and particle physics. Their inner composition still remains an open question. The extreme densities reached in NS cores might originate some exotic matter, such as hyperons, Bose-Einstein condensates or quark matter [1].

The two solar mass pulsars PSR J1614-2230 ($M = 1.908 \pm 0.016\ M_\odot$) and PSR J0348 + 0432 ($M = 2.01 \pm 0.04\ M_\odot$) [2] and MSP J0740 + 6620 [3], ($M = 2.14^{+0.10}_{-0.09} M_\odot$) impose tight constraints on the nuclear matter equation of state (EoS). Multimessenger astrophysics that combines astrophysical observations of different type, electromagnetic radiation, gravitational waves (GW) and different types of particles provide deeper insights on NS properties. The analysis by the LIGO/Virgo collaborations of the GW from the NS merger GW170817 gave us important information about the NS structure [4,5], e.g., an upper limit of the tidal deformability of a NS star, that allows us to set extra constraints on the high density EoS. Moreover, the detection of the gamma-ray burst (GRB) GRB170817A [6], and the electromagnetic transient AT2017gfo [7] that followed up the GW170817 event has further established constraints on the lower limit of the tidal deformability [8–12]. The Neutron Star Interior Composition Explorer (NICER) experiment is presently another important source of observational data that may shed some light into the structure of NS. Recently, two different teams of NICER have estimated the mass and radius of the millisecond-pulsar PSR J0030 + 0451 [13].

While massive pulsars rule out soft EoS at high densities, a too stiff EoS, which gives rise to large radii, is incompatible with the tidal deformability from GW observations [14]. The high density region of the EoS is thus severely constrained, which may exclude exotic, i.e., non-nucleonic, degrees of freedom inside NS, such as quark matter. However, the existence of a first order phase transition from hadronic to quark matter, depending on its properties, may balance the two features mentioned above and still explain the observational data [14]. Detecting observational signatures that indicate the presence of exotic matter inside neutrons stars is a major difficulty. For instance, it is hard to establish a clear physical distinction between a purely hadronic NS and one with a quark core solely from NS observables, such as the star mass, radius and tidal deformability. However, the presence of a first order phase transition between hadronic and quark matter can lead to observational signatures that could be exploited in more neutron star binary mergers observations, favoring the hypothesis of quark matter in the neutron star core [14–16].

One way to study quark degrees of freedom in NS matter is through effective models, which incorporate the most important properties and symmetries of the strong interactions. The Nambu–Jona-Lasinio (NJL) model is an widely used effective model of QCD. Some of its

[*]marcio.ferreira@uc.pt
[†]renan.pereira@student.uc.pt
[‡]cp@uc.pt

applications are the study of the phase diagram of QCD, the behavior of mesons at finite temperature and density and also to study of the possible existence of quark matter inside neutron stars [17–26]. The NJL model Lagrangian is built considering symmetry preserving interactions, specially chiral symmetry [27,28].

A possible approach to construct an hybrid EoS is the two model approach: one that describes the hadronic (confined) phase and a second model describing the quark (deconfined) phase. The matching of the two EoS may be carried out within different approaches, in particular considering local charge neutrality or global charge neutrality [1]. In the present approach we will consider a Maxwell construction to describe a first-order phase transition from hadron matter to a quark phase. This approach is considered to be quite realistic if the surface tension between hadron and quark matter, a still unknown quantity, is large. This methodology has been widely used, where an hadronic model and an independent quark model were considered, see [21,29–33]. Using the NJL model to describe the quark phase of a hybrid EoS, previous works have successfully predicted neutron stars with at least 2 $M_\odot$ [22,32]. The presence of the vector-isoscalar interaction was shown to be very important in stiffening the EoS to sustain 2 $M_\odot$. The inclusion of 8-quark interactions in the scalar and in the vector-isoscalar channel within the two-flavor NJL model was explored in [29,30] in the context of hybrid stars. In [34], local and nonlocal NJL models with vector interaction were seen to typically give no hybrid stars (or just small quark branches). The 8-quark vector-isoscalar interaction should be interpreted as an effective interaction that includes nonlinear terms to take into account medium effects in a spirit similar to the one that took Brown and Rho to propose their scaling effective Lagrangians in a dense medium in [35]. The interaction vector-isoscalar 8-quark interaction in the NJL model is equivalent to the nonlinear $(\omega^\mu\omega_\mu)^2$ term introduced in the Lagrangian density of the relativistic nuclear model TM1 [36,37] to weaken effects of the repulsive ω-meson contribution at high densities and reproduce DBHF results. The inclusion of eight quark interactions may be understood as an effective way of considering density dependent coupling constants at large densities. An alternative approach is to include the density dependence in quark models through the introduction of a chemical potential dependence [38–41].

It has been shown by several authors that the onset of the Δ may compete with the onset of hyperons, and due to its large isospin and the still lack of information to fix the coupling constants these particles may set in at densities below the onset of hyperons, just above saturation density [42–45]. In particular, the onset of Δs may occur in low mass stars making compatible relativistic mean-field models with the constraint set by GW170917 on the tidal deformability. In the present work, we will show an alternative scenario and will show that the onset of quarks at densities below twice saturation density may also have a similar effect of pushing down the tidal deformability of stars with masses $\sim 1.4\ M_\odot$ or below.

Using a constant-sound-speed parametrization for the high-density EoS region [46,47], the authors concluded that for a strong first-order phase transition to quark matter to be compatible with $M_{\max} > 2\ M_\odot$ requires a large speed of sound in the quark phase, $v_s^2 \gtrsim 0.5$ for soft hadronic EoS and $v_s^2 \gtrsim 0.4$ for stiff hadronic EoS. Using the same formalism, the work [48] points in the same direction: strong repulsive interactions in quark matter are required to support the NS masses $M \gtrsim 2.0\ M_\odot$.

In [49], the authors studied the possibility of occurrence of stars with quark cores, imposing well known constraints, both observational and theoretical ab-initio calculations, to a large set of EoS built using metamodels parametrized by the speed of sound. They propose that 1.4 $M_\odot$ stars are compatible with hadronic stars. Besides, they infer that massive stars with a mass $\approx 2\ M_\odot$ and a speed of sound not far from the conformal limit will have large quark cores. We would like to understand whether it is possible to arrive to similar conclusions starting from a set of quark matter EoS that satisfy a given number of constraints set by properties of mesons in the vacuum which, also have been derived from a model with intrinsic chiral symmetry.

To attain this aim, we will work in the framework of the three-flavor NJL model, and we will analyze the effect of 4-quark and 8-quark vector-isoscalar interactions in hadron-quark hybrid EoS. Having as framework the NJL functional with a 8-quark vector-isoscalar interaction allows for the generation of hybrid EoS that satisfy nuclear matter constraints and observational constraints. Using this strategy we avoid meta-modeling the EoS with polytropes or the speed of sound approaches [49,50] and we use a functional based on a relativistic and chiral symmetric framework. NJL models typically give rather low values for the speed of sound in the quark matter phase ($v_s^2 \sim 0.2$–0.3) and have a small dependence on the density. Furthermore, the speed of sound is quite insensitive to the NJL model parameters Λ, $m_{u,d}$, m_s, G_S, G_D, i.e., the cutoff, current masses and couplings of the scalar and t'Hooft terms. We will investigate the impact of the vector interactions in the speed-of-sound and in the quark phase and thus on the stability of hybrid stars sequences. Moreover, exploring these additional interactions, we will analyze the possibility of having quark cores in light NS and, at the same time, fulfill all observational constraints.

This paper is organized as follows: in Sec. II the quark model is detailed. The results are presented in Sec. III followed by our conclusions, in Sec. IV.

II. MODEL AND FORMALISM

The $\mathrm{SU}(3)_f$ NJL Lagrangian density, including four and six scalar-pseudoscalar interactions and four and eight vector-isoscalar interactions is

$$\begin{aligned}\mathcal{L} &= \bar{\psi}(i\partial\!\!\!/ - \hat{m} + \hat{\mu}\gamma^0)\psi \\ &+ G_S \sum_{a=0}^{8} [(\bar{\psi}\lambda^a\psi)^2 + (\bar{\psi} i\gamma^5 \lambda^a \psi)^2] \\ &- G_D[\det(\bar{\psi}(1+\gamma_5)\psi) + \det(\bar{\psi}(1-\gamma_5)\psi)] \\ &- G_\omega[(\bar{\psi}\gamma^\mu\lambda^0\psi)^2 + (\bar{\psi}\gamma^\mu\gamma_5\lambda^0\psi)^2] \\ &- G_{\omega\omega}[(\bar{\psi}\gamma^\mu\lambda^0\psi)^2 + (\bar{\psi}\gamma^\mu\gamma_5\lambda^0\psi)^2]^2. \end{aligned} \tag{1}$$

The diagonal matrices $\hat{m} = \mathrm{diag}(m_u, m_d, m_s)$ and $\hat{\mu} = \mathrm{diag}(\mu_u, \mu_d, \mu_s)$ are the quark current masses and chemical potential matrices, respectively. The matrices λ^a with components $a = 1, 2 \ldots 8$, are the Gell-Mann matrices of the SU(3) group while, the zero component, is a matrix proportional to the identity matrix, $\lambda^0 = \sqrt{2/3}\mathbb{1}$. The quark field has N_f-components in flavor space.

The NJL model is nonrenormalizable in four dimensional space-time. Hence some regularization procedure must be employed in order to regularize the integrals. Alongside with the Matsubara formalism to derive the thermodynamical potential, we are going to regularize the integrations using the 3-momentum cutoff regularization.

The multi-quark interactions considered are all chiral symmetry preserving. The four scalar and pseudoscalar quark interactions are present in the original formulation of the NJL model and are essential to incorporate spontaneous chiral symmetry breaking in the model. The 't Hooft determinant for three quark flavours corresponds to a six quark interaction which incorporates the explicit $U_A(1)$ symmetry breaking in the model. Incorporating vector interaction in the model has been found to be necessary to model the medium to high density behavior of the EoS and predict $2\,M_\odot$ neutron stars. The inclusion of all possible chiral-symmetric set of eight quark vector interactions was performed in [51] in order to study the masses of the lowest spin-0 and spin-1 meson states. Following previous works, the vector-isoscalar quark interactions have been shown to be essential to build $2\,M_\odot$ neutron stars.

In the present work, we will restrict our analysis to four and eight vector-isoscalar quark interactions and study their influence on the EoS of hybrid neutron stars. These vector interactions have coupling constants, G_ω and $G_{\omega\omega}$ respectively. In general, both of these couplings can be fixed in the vacuum by fitting the omega meson mass. Indeed, while the masses and decay constants of the scalar/pseudoscalar mesons do not depend explicitly on the G_ω and $G_{\omega\omega}$ couplings, parametrizing the model using the omega-meson mass would affect the values of the interaction couplings, the quark current masses and cutoff, see [28]. However, in the present work we are not interested in studying the behavior of vector mesons. The vector interactions are used as a way to parametrize unknown degrees of freedom that can make the EOS softer or stiffer at medium to large densities. Indeed, as discussed in the literature [28,52], the vector-isoscalar terms are proportional to density degrees of freedom and their couplings might be density dependent. Hence, to take into account the possible in-medium dependence of the vector couplings G_ω and $G_{\omega\omega}$, we will not fix their magnitudes in the vacuum and leave them as free parameters. As in our previous works [32], we will study different models defined by different values for the ratios $\xi_\omega = G_\omega/G_S$ and $\xi_{\omega\omega} = G_{\omega\omega}/G_S^4$.

The thermodynamical potential of the NJL model is calculated in the mean field (MF) approximation, where the product between quark bilinear operators are linearized around their mean field values, and a linear Lagrangian density can be obtained (for more details on the linear product between N operators see [53]). The quark fields can then be integrated out.

Using the Matsubara formalism and the linearized Lagrangian density, the MF thermodynamical potential of the NJL model, Ω, is derived from the lagrangian written in Eq. (1). For finite temperature and chemical potential it can be written as:

$$\begin{aligned}\Omega - \Omega_0 &= 2G_S(\sigma_u^2 + \sigma_d^2 + \sigma_s^2) - 4G_D\sigma_u\sigma_d\sigma_s \\ &- \frac{2}{3}G_\omega(\rho_u + \rho_d + \rho_s)^2 - \frac{4}{3}G_{\omega\omega}(\rho_u + \rho_d + \rho_s)^4 \\ &- 2TN_c \sum_{i=u,d,s} \int_0^\Lambda \frac{\mathrm{d}^3p}{(2\pi)^3} \ln\left(1 + \mathrm{e}^{-(E_i+\tilde{\mu}_i)/T}\right) \\ &- 2TN_c \sum_{i=u,d,s} \int_0^\Lambda \frac{\mathrm{d}^3p}{(2\pi)^3} \ln\left(1 + \mathrm{e}^{-(E_i-\tilde{\mu}_i)/T}\right) \\ &- 2N_c \sum_{i=u,d,s} \int_0^\Lambda \frac{\mathrm{d}^3p}{(2\pi)^3} E_i. \end{aligned} \tag{2}$$

The constant Ω_0 is calculated in such a way that the potential vanishes in the vacuum. Also, $E_i = \sqrt{p^2 + M_i^2}$ and σ_i and ρ_i are the condensate and density of the quarks with flavor i, respectively.

For $i \neq j \neq k \in \{u, d, s\}$, the effective mass, M_i, and effective chemical potentials, $\tilde{\mu}_i$, are found to be

$$M_i = m_i - 4G_S\sigma_i + 2G_D\sigma_j\sigma_k, \tag{3}$$

$$\tilde{\mu}_i = \mu_i - \frac{4}{3}G_\omega(\rho_i + \rho_j + \rho_k) - \frac{16}{9}G_{\omega\omega}(\rho_i + \rho_j + \rho_k)^3. \tag{4}$$

In the MF approximation the thermodynamical potential must be stationary with respect to the effective mass, M_i, and effective chemical potentials [28], $\tilde{\mu}_i$, i.e.,

$$\frac{\partial\Omega}{\partial M} = \frac{\partial\Omega}{\partial\tilde{\mu}} = 0. \tag{5}$$

Applying these stationary conditions to the thermodynamical potential yields a closed expression for the quark

condensate, σ_i, and density, ρ_i. For the explicit expressions see [54].

The quark sector of the cold hybrid EoS can be easily calculated from Eq. (2) in the $T = 0$ limit. The pressure and energy density are given by

$$P = -\Omega, \tag{6}$$

$$\epsilon = -P + \sum_i \mu_i \rho_i. \tag{7}$$

Aside from the free vector couplings, G_ω and $G_{\omega\omega}$, the remaining parameters of the model are fixed in order to reproduce the values of some meson masses and decay constants. The used parameter set can be found in Table I. In Table II we present the values of some meson masses and leptonic decay constants within the parameter set in Table I and the respective experimental values.

The NJL model pressure and energy density are defined up to a constant B, analogous to the MIT bag constant [21]. It it essential in building hybrid EoS that sustain two-solar mass neutrons stars. In [21,32], B was fixed by requiring that the deconfinement occurs at the same baryonic chemical potential as the chiral phase transition. More recently in [48], an effective bag constant was also used to control the density at which the phase transition from hadron to quark matter happened. In the presence of a finite bag constant, the quark EoS is modified by $P \to P + B$ and $\epsilon \to \epsilon - B$. Hence the NJL quark EoS will be defined by three parameters: the model vector coupling ratios, $\xi_\omega = G_\omega/G_S$ and $\xi_{\omega\omega} = G_{\omega\omega}/G_S^4$ and the bag constant B.

TABLE I. Parameters of the NJL model used in the present work: Λ is the model cutoff, $m_{u,d}$ and m_s are the quark current masses, G_S and G_D are coupling constants. $M_{u,d}$ and M_s are the resulting constituent quark masses in the vacuum. This parameter set yields, in the vacuum, a light quark condensate of $\langle \bar{q}_l q_l \rangle^{1/3} = -243.9$ MeV and strange quark condensate of $\langle \bar{q}_s q_s \rangle^{1/3} = -262.9$ MeV.

Λ [MeV]	$m_{u,d}$ [MeV]	m_s [MeV]	$G_S\Lambda^2$	$G_D\Lambda^5$	$M_{u,d}$ [MeV]	M_s [MeV]
623.58	5.70	136.60	1.67	13.67	332.2	510.7

TABLE II. The masses and decay constants of several mesons within the model and the respective experimental values.

	NJL SU(3)	Experimental [55]
$m_{\pi^\pm}$ [MeV]	139.6	139.6
$f_{\pi^\pm}$ [MeV]	92.0	92.2
$m_{K^\pm}$ [MeV]	493.7	493.7
$f_{K^\pm}$ [MeV]	96.4	110.4
m_η [MeV]	515.6	547.9
$m_{\eta'}$ [MeV]	957.8	957.8

For the hadronic part of the hybrid stars we use the DDME2 model [56]. This is a relativistic mean-field model with density dependent couplings that describes two solar mass stars and satisfies a well established set of nuclear matter and finite nuclei constraints [57,58], including the constraints set by the *ab initio* calculations for neutron matter using a chiral effective field theoretical approach [59]. This has been the low density constraint set in [49].

III. RESULTS

Herein, we analyze the effect of the vector-isoscalar couplings $\xi_\omega = G_\omega/G_S$ and $\xi_{\omega\omega} = G_{\omega\omega}/G_S^4$ on the hybrid EoS and respective NS properties. The effect of the bag constant B was already studied in [18,21–26,32,54,60–62], where it was found that the onset of quark matter in the hybrid EoS happens at lower densities as B increases. Although we have explored several values for B, we have decided to keep it fixed in the following analysis to $B = 10$ MeV/fm^3. Increasing B shifts the hadron-quark transition to lower densities as discussed in [54]. The value of B should be constrained from below imposing that no quark matter exists for symmetric nuclear matter at saturation density. We have chosen a value that does not predict unrealistic physical scenarios such as quark matter at too low density and still allows for the presence of a quite large quark cores in low mass stars, as will be shown in the following. As free parameters, we consider $\{\xi_\omega, \xi_{\omega\omega}\}$ which give a considerable flexibility to span a wide range of EoS with the required properties. In the following, charge-neutral neutron star matter in β–equilibrium, with a first-order phase transition (via a Maxwell construction) from hadronic matter to quark matter happens, is studied. It is important to include both terms because they play a different role: the G_ω term makes the EoS harder, a necessary condition to get two solar mass stars. However, if the EoS is too stiff no transition to quark matter is predicted. This can still be partially regulated with the inclusion of the bag pressure B but only allows for small quark cores. The effect of the $G_{\omega\omega}$ term becomes more important at large densities. As a consequence, the stellar matter enters the quark phase as a quite soft EoS, but, as the density increases, the effect of the $G_{\omega\omega}$ term becomes stronger and stronger, allowing for massive and stable stars with a large quark core.

The main effect of the 4-quark vector term is to stiffen the quark EoS and shift the onset of quark matter to larger densities as discussed in [26,32]. Moreover, the larger the coupling constant, ξ_ω the smaller the quark core. This behavior has been described considering a constant speed of sound model for the quark phase [63].

Let us now analyze how $\xi_{\omega\omega}$ affects the quark matter EoS. Figure 1 shows the pressure (right) and the speed of sound squared (left) as a function of baryonic density, $n = (\rho_u + \rho_d + \rho_s)/3$, for $\xi_\omega = 0$ (herein, we use $c = 1$). The speed of sound, $v_s^2 = dp/d\epsilon$, characterizes how stiff

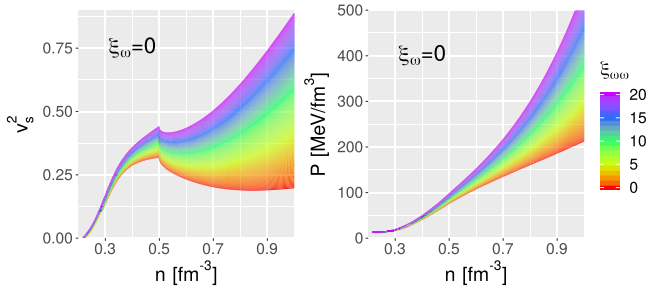

FIG. 1. The speed of sound (left) and pressure (right) as a function of the baryonic density for quark matter with $\xi_\omega = 0$. The color scale indicates the $\xi_{\omega\omega}$ value.

the EoS is. It is clear from both panels that the 8-quark term, characterized by the coupling $\xi_{\omega\omega}$, allows the quark EoS to become stiffer so that a larger quark core will be sustained in the hybrid NS: this term gives rise to a density dependent speed of sound that increases nonlinearly with density. The main role of $\xi_{\omega\omega}$ is played at large densities: it affects in a much smaller extension the onset of quark matter than the ξ_ω coupling. This is clearly seen in Fig. 2, where the onset density of quark matter, for each hybrid EoS, is shown by a color degrade in terms of the parameters $\xi_{\omega\omega}$ and ξ_ω. The change of color is only slightly dependent on $\xi_{\omega\omega}$.

The sudden decrease of the speed of sound v_s^2 at $n \approx 0.5$ fm^{-3} is due to the onset of strangeness. Note, however, that the appearance of the strange quark occurs via a crossover and thus in a continuous way. Since the vector terms introduced are flavor invariant [28], the onset of strangeness does not depend of the vector terms and is completely defined by the properties of the model shown in Table I. The amount of strangeness inside the star, will, therefore, be determined by the central density that depends on both vector terms.

We plot in Fig. 3 our set of EoS on a pressure vs energy density graph for $\xi_\omega = 0$, and include in the background the acceptable region of EoS defined in [49]. We conclude that

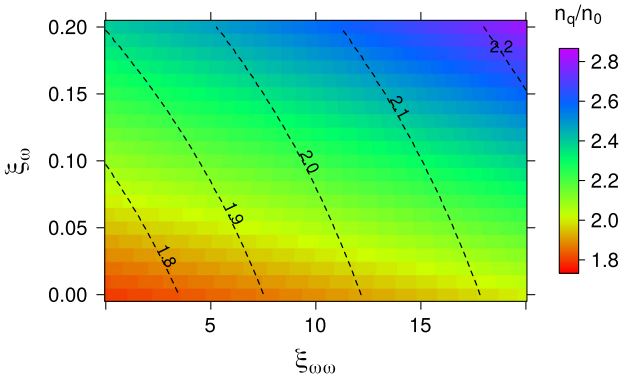

FIG. 2. Onset density of quark matter, n_q (in units of saturation density, $n_0 = 0.155$ fm^{-3}), as a function of both ξ_ω and $\xi_{\omega\omega}$. The dashed lines represent the value of the maximum NS mass [in $M_\odot$] reached by each hybrid EoS, defined by $(\xi_\omega, \xi_{\omega\omega})$.

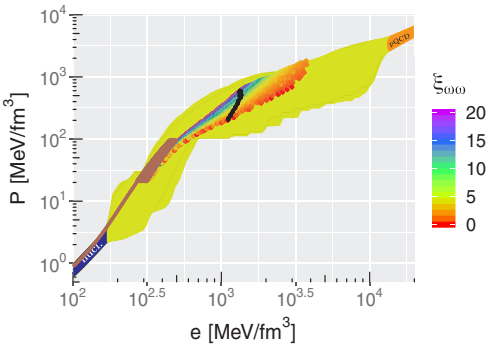

FIG. 3. The EoS used in the present study in pressure vs energy density. The color scale refers to the parameter $\xi_{\omega\omega}$. At low densities the DDME2 EoS is represented followed by the hadron-quark phase transition at constant pressure (Maxwell construction). All EoS shown are causal. On the background the contours of the region defined in [49] for the acceptable EoS that interpolate between the neutron matter EoS determined for a chiral effective field theory approach in [59] and the pQCD EoS calculated in [64]. The black dots identify the maximum mass stars.

our set of EoS covers a quite large fraction of the proposed region. The red color indicates a region with a speed of sound $v_s^2 \lesssim 0.3$ as shown in Fig. 1. Our most massive stars (purple color) lie close to the boarder of the region and are associated with a central speed of sound well above the conformal limit, which can be as large as 0.9c. Some interesting conclusions are: (a) our set of EoS also defines a change of slope. This could be due to the fact that we work with a model with chiral symmetry incorporated. This kind of knee is also present in other studies [50]; (b) we get low mass stars with a quark core below the knee; (c) our heaviest stars with a large quark core have a speed of sound far from the conformal limit; (d) the red dots identify EoS with a speed of sound close to the conformal limit and lie in the center of the region as obtained in [49]; (e) the vector interactions considered in this work do not span the whole region of the Fig. 3. Including extra four and eight quark vector interactions, for instance in the scalar and vector-isovector channels, may increase this region. This is left as future work.

In order to study the NS properties we have integrated the Tolmann-Oppeheimer-Volkof (TOV) equations [65,66] and the tidal deformabilities Λ are calculated as in [67–69]. Figure 4 shows the $M(R)$ diagram for each hybrid EoS, parametrized by $(\xi_\omega, \xi_{\omega\omega})$. For the sake of clarity, we have fixed ξ_ω in each panel: $\xi_\omega = 0.0$ (left), $\xi_\omega = 0.1$ (center), and $\xi_\omega = 0.2$ (right). The color scale encodes the value of $\xi_{\omega\omega}$. The effect of ξ_ω is clear: as its value increases, quarks appear at larger masses and shorter quark star branches, which reach higher $M_{\max}$, are obtained. As expected, given that both represent repulsive interactions, $\xi_{\omega\omega}$ shows the same trend as ξ_ω. Higher values of $\xi_{\omega\omega}$ originate longer quark branches capable of reproducing more massive NS. The most interesting cases occur for smaller values of ξ_ω

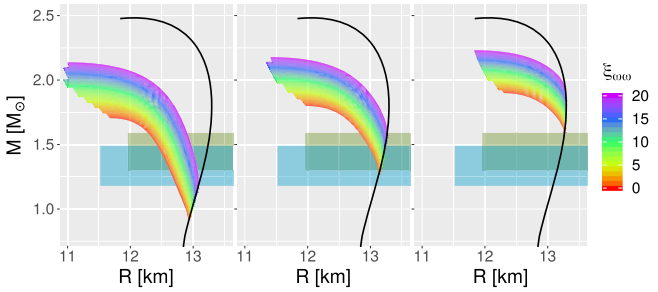

FIG. 4. $M(R)$ diagrams for $\xi_\omega = 0$ (left), $\xi_\omega = 0.1$ (center), and $\xi_\omega = 0.2$ (right). The color scale indicates the $\xi_{\omega\omega}$ value and the black line represents the purely hadronic sequence. The bag constant is fixed at $B = 10\ \mathrm{MeV/fm^3}$. The colored regions indicate the (M, R) constraints obtained by two independent analysis using the NICER x-ray data from the millisecond pulsar PSR J0030 + 0451 [13,70].

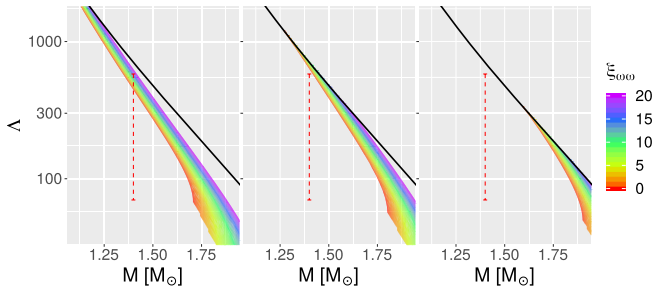

FIG. 5. $\Lambda(M)$ diagrams for $\xi_\omega = 0$ (left), $\xi_\omega = 0.1$ (center), and $\xi_\omega = 0.2$ (right). The color scale indicates the $\xi_{\omega\omega}$ value and the black line represents the purely hadronic sequence. The bag constant is fixed at $B = 10\ \mathrm{MeV/fm^3}$. The dashed red line indicates the constraint $70 < \Lambda_{1.4\ M_\odot} < 580$ (90% level) from the GW170817 event [71].

and for considerable values of $\xi_{\omega\omega}$, see left and center panels. Under these conditions, quarks are already present inside light NS, $M > 0.9\ M_\odot$, and it is still possible to attain quite massive and compact NS, $M \approx 2.2\ M_\odot$ and $R \approx 11$ km. For $\xi_{\omega\omega} > 10$, hybrid NS with $M > 1.9\ M_\odot$ that predict already some quark content for $M \approx 1.0\ M_\odot$ NS are possible.

We have represented two shaded regions in Fig. 4 that indicate the (M, R) constraints obtained by two independent analysis using the NICER x-ray data from the millisecond pulsar PSR J0030 + 0451 [13,70]. The set of hybrid EoS in the present work are in good agreement with both constraints.

The $\Lambda(R)$ diagrams are shown in Fig. 5. Like in Fig. 4, we show three panels: $\xi_\omega = 0.0$ (left), $\xi_\omega = 0.1$ (center), and $\xi_\omega = 0.2$ (right). The red dashed line represents the constraint $70 < \Lambda_{1.4\ M_\odot} < 580$ (90% level) obtained from the GW170817 event [71]. We see that, with the combination of low ξ_ω and high $\xi_{\omega\omega}$, it is possible to generate an hybrid EoS that softens the hadronic EoS (solid black line) at low baryonic densities, and satisfies the GW170817 $\Lambda_{1.4\ M_\odot}$ constraint. Another interesting result is that the radius of the heaviest stable NS, $R_{\max}$, is quite sensitive to the $\xi_{\omega\omega}$ value, and it is possible to predict sequences in the $\Lambda(R)$ diagram that clearly deviate from the purely hadronic EoS one. Small values of Λ for a low/intermediate mass star could be an important signature indicating the presence of quark matter in NS, which would be accessible through observational results on (M_i, R_i, Λ_i).

In Fig. 6, we show how the central density, $n_{\max}$ at the maximum NS, $M_{\max}$, depends on $(\xi_\omega, \xi_{\omega\omega})$. The overall effect of ξ_ω is to decrease the central density of $M_{\max}$, while $\xi_{\omega\omega}$ shows a clear nonmonotonic impact on $n_{\max}$. The maximum value of $n_{\max}$ is reached for $\xi_\omega = 0$ and $\xi_{\omega\omega} \approx 11$. This is already seen in Fig. 4 (left panel), where the $R_{\max}$ shows a nonmonotonic behavior: it increases up to $\xi_{\omega\omega} = 10$ and then starts to decrease for higher $\xi_{\omega\omega}$ values.

Since the onset of the s-quark occurs at $n \approx 0.5\ \mathrm{fm^{-3}}$ independently of the vector interaction, as we have seen before, we conclude that all stars have some fraction of s-quarks. However, if $\xi_\omega > 0.1$ the amount of strangeness is quite small. This behavior has also been found in hadronic matter with hyperons: if the coupling to the vector mesons is strong the strangeness content of the star is small [72,73]. It is interesting, however, to realize that the 8-quark term stiffens the EoS but still allows very large central baryonic densities, and, as a consequence, a large strangeness content.

In Fig. 7, we display the speed of sound squared, v_s^2, attained at the central density of the heavier NS ($M_{\max}$) for each hybrid EoS, i.e., $v_s^2(n_{\max})$, which is a function of $(\xi_\omega, \xi_{\omega\omega})$. v_s^2 is very sensitive to $\xi_{\omega\omega}$ and is only slightly affected by ξ_ω. To reach massive NS cores, it is crucial to have large v_s^2 values. The quark core of $M \approx 1.8\ M_\odot$ in Figure 8, is possible only because the star has a very stiff quark matter phase, with $v_s^2 \approx 0.93$.

Let us now analyze how the quark core size depends on $(\xi_\omega, \xi_{\omega\omega})$. Figure 8 displays both the mass of the quark

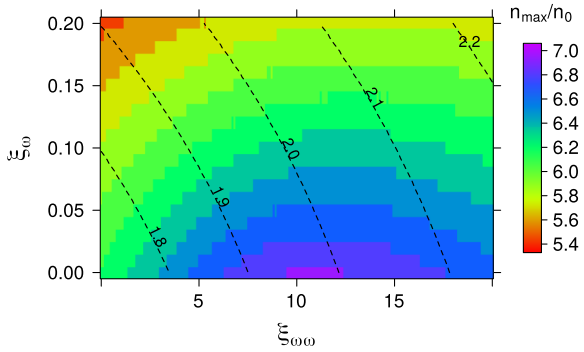

FIG. 6. Central density at the maximum NS mass, $n_{\max}$ [in units of saturation density, $n_0 = 0.155\ \mathrm{fm^{-3}}$], as a function of both ξ_ω and $\xi_{\omega\omega}$. The dashed lines represent the value of the maximum NS mass [in $M_\odot$] reached by each hybrid EoS, defined by $(\xi_\omega, \xi_{\omega\omega})$.

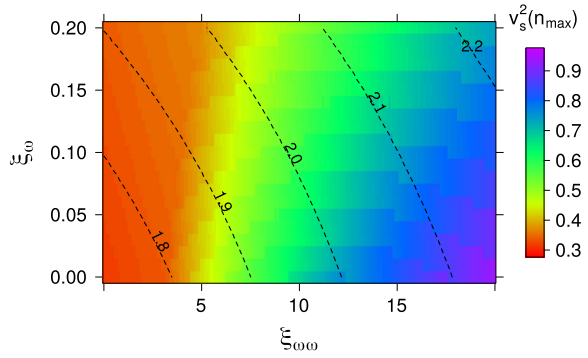

FIG. 7. Speed of sound at the central density of the most massive stable NS, $v_s^2(n_{\max})$, as a function of both ξ_ω and $\xi_{\omega\omega}$. The dashed lines represent the value of the maximum NS mass [in $M_\odot$] reached by each hybrid EoS, defined by $(\xi_\omega, \xi_{\omega\omega})$.

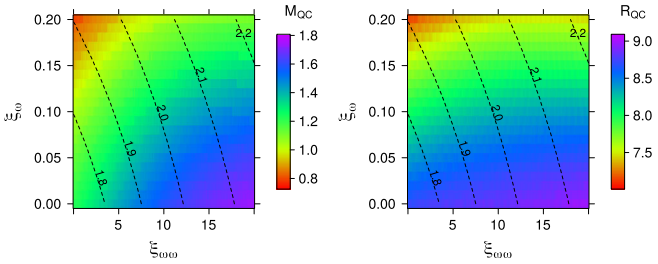

FIG. 8. The quark core mass M_{QC} [in $M_\odot$] (left) and radius R_{QC} [in km] (right) as a function of both ξ_ω and $\xi_{\omega\omega}$. The dashed lines represent the value of the maximum NS mass [in $M_\odot$] reached by each hybrid EoS, defined by $(\xi_\omega, \xi_{\omega\omega})$.

core, M_{QC} (right panel), and the radius, R_{QC} (left panel), as a function of $(\xi_\omega, \xi_{\omega\omega})$. We further indicate the maximum mass reached by each hybrid stars through contour lines as before (black dashed lines). For a fixed ξ_ω value, M_{QC} increases with $\xi_{\omega\omega}$, reaching a heavier quark core for low ξ_ω and high $\xi_{\omega\omega}$. This is precisely when the central density is the largest. On the other hand, for a fixed $\xi_{\omega\omega}$ value, M_{QC} decreases as the value of ξ_ω gets bigger. Therefore, the extremes of $M_{QC}(\xi_\omega, \xi_{\omega\omega})$ lie in opposite regions: the lighter quark core, $M \approx 0.8\ M_\odot$, is found for $(\xi_\omega = 0.2, \xi_{\omega\omega} = 0)$ while the heavier, $M \approx 1.8\ M_\odot$, is generated for $(\xi_\omega = 0, \xi_{\omega\omega} = 20)$. Actually, a quark core of $M \approx 1.8\ M_\odot$ is generated in a region where $M_{\max} \approx 2.1\ M_\odot$, showing that 85% of the star has quark degrees of freedom. Even though R_{QC} displays a similar trend as M_{QC}, there is a greater sensitivity to ξ_ω than $\xi_{\omega\omega}$. Even for low $\xi_{\omega\omega}$ values, the quark core radii can reach values as high as 9 km, although two solar mass stars are not attained for these values. The contour lines representing $M_{\max}$ reflect a much stronger dependence on $\xi_{\omega\omega}$ than on ξ_ω.

IV. CONCLUSIONS

In this work we have analyzed the effect of 4-quark and 8-quark vector-isoscalar interactions in hadron-quark hybrid EoS within the three flavor NJL model. Each hybrid EoS consists of charge-neutral matter in β–equilibrium, in which a first-order phase transition from hadronic to quark matter is present. We have analyzed how the stability of hybrid stars sequences and their properties depend on the four and eight vector-isoscalar couplings, $\xi_\omega = G_\omega/G_S$ and $\xi_{\omega\omega} = G_{\omega\omega}/G_S^4$.

From the density dependence of the speed of sound of quark matter, one clearly recognizes the stiffening effect of both interactions. This behavior imprints interesting features in the sequences of stable star in the $M(R)$ diagram. We show that the size of the quark star branch is quite sensitive to both couplings, particularly to the $\xi_{\omega\omega}$ coupling. With a small value for ξ_ω, there is a range of $\xi_{\omega\omega}$ values that predict quark matter in light NS, $\sim 1\ M_\odot$, and, at the same time, are able to sustain a quark core in quite massive NS, i.e., $\sim 2.1\ M_\odot$. Furthermore, the radius of the heaviest stable NS, $R_{\max}$, is highly dependent on the strength of $\xi_{\omega\omega}$, leading to a considerable decrease of $R_{\max}$ as the coupling increases. As a consequence, for a hybrid EoS a considerable deviation from the purely hadronic matter EoS prediction for the tidal deformability $\Lambda(M)$ is obtained. This occurs even for moderate NS masses, $\sim 1.4\ M_\odot$, in accordance with the astrophysical constraints from NICER and LIGO/Virgo observations.

We have also discussed how the size of the quark core depends on ξ_ω and $\xi_{\omega\omega}$. We have concluded that, for a fixed ξ_ω value, M_{QC} increases with $\xi_{\omega\omega}$. While lighter quark cores, $\sim 0.8\ M_\odot$, are predicted for $(\xi_\omega = 0.2, \xi_{\omega\omega} = 0)$, the heaviest cores, $\sim 1.8\ M_\odot$, are generated in the opposite regime, i.e., $(\xi_\omega = 0, \xi_{\omega\omega} = 20)$. Quite massive quark cores, $\sim 1.8\ M_\odot$, are predicted for hybrid EoS in each $M_{\max} \approx 2.1\ M_\odot$, showing that there are quark degrees of freedom in 85% of the star.

Concerning the conclusions drawn in [49], we obtain some similar results, in particular, we are able to describe two solar mass stars with a central speed of sound squared below 0.4, but more massive stars require larger central values for the speed of sound. However, some other aspects in our study differ from the ones discussed in [49]. We have obtained low mass stars with a quark core, and we can describe very massive stars with large quark cores and a speed of sound far from the conformal limit.

A low mass NS with a quark core would be confirmed if together with the BNS tidal deformability and mass, also the dominant post-merger GW frequency f_{peak} would be measured. In [74] it was shown that this frequency would identify a first-order phase transition. In the presence of a first order phase transition the f_{peak} comes at a much larger frequency: the larger the baryonic density gap at the phase transition the larger the frequency.

ACKNOWLEDGMENTS

This work was partially supported by national funds from FCT (Fundação para a Ciência e a Tecnologia, I.P,

Portugal) under the IDPASC Ph.D. program (International Doctorate Network in Particle Physics, Astrophysics and Cosmology), with the Grant No. PD/BD/128234/2016 (R. C. P.), under the Projects No. UID/FIS/04564/2019, No. UID/04564/2020, and No. POCI-01-0145-FEDER-029912 with financial support from Science, Technology and Innovation, in its FEDER component, and by the FCT/MCTES budget through national funds (O. E.).

[1] N. Glendenning, *Compact Stars: Nuclear Physics, Particle Physics and General Relativity*, Astronomy and Astrophysics Library (Springer, New York, 2012).
[2] J. Antoniadis *et al.*, Science **340**, 1233232 (2013).
[3] H. T. Cromartie *et al.*, Nat. Astron. 439 (2019).
[4] B. P. Abbott *et al.* (The LIGO Scientific and the Virgo Collaborations), Phys. Rev. Lett. **119**, 161101 (2017).
[5] B. A. Abbott *et al.* (The LIGO Scientific and the Virgo Collaborations), Phys. Rev. Lett. **121**, 161101 (2018).
[6] B. P. Abbott *et al.* (LIGO Scientific, Virgo, Fermi-GBM, and INTEGRAL Collaborations), Astrophys. J. **848**, L13 (2017).
[7] B. P. Abbott *et al.* (LIGO Scientific, Virgo, Fermi GBM, INTEGRAL, IceCube, AstroSat Cadmium Zinc Telluride Imager Team, IPN, Insight-Hxmt, ANTARES, Swift, AGILE Team, 1M2H Team, Dark Energy Camera GW-EM, DES, DLT40, GRAWITA, Fermi-LAT, ATCA, ASKAP, Las Cumbres Observatory Group, OzGrav, DWF (Deeper Wider Faster Program), AST3, CAASTRO, VINROUGE, MASTER, J-GEM, GROWTH, JAGWAR, CaltechNRAO, TTU-NRAO, NuSTAR, Pan-STARRS, MAXI Team, TZAC Consortium, KU, Nordic Optical Telescope, ePESSTO, GROND, Texas Tech University, SALT Group, TOROS, BOOTES, MWA, CALET, IKI-GW Follow-up, H.E.S.S., LOFAR, LWA, HAWC, Pierre Auger, ALMA, Euro VLBI Team, Pi of Sky, Chandra Team at McGill University, DFN, ATLAS Telescopes, High Time Resolution Universe Survey, RIMAS, RATIR, SKA South Africa/MeerKAT Collaborations), Astrophys. J. **848**, L12 (2017).
[8] D. Radice, S. Bernuzzi, W. Del Pozzo, L. F. Roberts, and C. D. Ott, Astrophys. J. **842**, L10 (2017).
[9] D. Radice, A. Perego, F. Zappa, and S. Bernuzzi, Astrophys. J. **852**, L29 (2018).
[10] A. Bauswein, N.-U. Friedrich Bastian, D. Blaschke, K. Chatziioannou, J. A. Clark, T. Fischer, H.-T. Janka, O. Just, M. Oertel, and N. Stergioulas, AIP Conf. Proc. **2127**, 020013 (2019).
[11] M. W. Coughlin *et al.*, Mon. Not. R. Astron. Soc. **480**, 3871 (2018).
[12] Y.-Z. Wang, D.-S. Shao, J.-L. Jiang, S.-P. Tang, X.-X. Ren, F.-W. Zhang, Z.-P. Jin, Y.-Z. Fan, and D.-M. Wei, Astrophys. J. **877**, 2 (2019).
[13] T. E. Riley, A. L. Watts, S. Bogdanov, P. S. Ray, R. M. Ludlam, S. Guillot, Z. Arzoumanian, C. L. Baker, A. V. Bilous, D. Chakrabarty, K. C. Gendreau, A. K. Harding, W. C. G. Ho, J. M. Lattimer, S. M. Morsink, and T. E. Strohmayer, Astrophys. J. **887**, L21 (2019).
[14] M. G. Alford, S. Han, and K. Schwenzer, J. Phys. G **46**, 114001 (2019).
[15] E. R. Most, L. J. Papenfort, V. Dexheimer, M. Hanauske, S. Schramm, H. Stöcker, and L. Rezzolla, Phys. Rev. Lett. **122**, 061101 (2019).
[16] L. R. Weih, M. Hanauske, and L. Rezzolla, Phys. Rev. Lett. **124**, 171103 (2020).
[17] K. Schertler, S. Leupold, and J. Schaffner-Bielich, Phys. Rev. C **60**, 025801 (1999).
[18] M. Hanauske, L. Satarov, I. Mishustin, H. Stoecker, and W. Greiner, Phys. Rev. D **64**, 043005 (2001).
[19] M. Baldo, M. Buballa, F. Burgio, F. Neumann, M. Oertel, and H. Schulze, Phys. Lett. B **562**, 153 (2003).
[20] D. Menezes and C. Providencia, Phys. Rev. C **68**, 035804 (2003).
[21] G. Pagliara and J. Schaffner-Bielich, Phys. Rev. D **77**, 063004 (2008).
[22] L. Bonanno and A. Sedrakian, Astron. Astrophys. **539**, A16 (2012).
[23] C. H. Lenzi and G. Lugones, Astrophys. J. **759**, 57 (2012).
[24] K. Masuda, T. Hatsuda, and T. Takatsuka, Prog. Theor. Exp. Phys. **2013**, 073D01 (2013).
[25] T. Klähn, R. Łastowiecki, and D. B. Blaschke, Phys. Rev. D **88**, 085001 (2013).
[26] D. Logoteta, C. Providência, and I. Vidaña, Phys. Rev. C **88**, 055802 (2013).
[27] T. Hatsuda and T. Kunihiro, Phys. Rep. **247**, 221 (1994).
[28] M. Buballa, Phys. Rep. **407**, 205 (2005).
[29] S. Benic, Eur. Phys. J. A **50**, 111 (2014).
[30] S. Benic, D. Blaschke, D. E. Alvarez-Castillo, T. Fischer, and S. Typel, Astron. Astrophys. **577**, A40 (2015).
[31] A. Zacchi, M. Hanauske, and J. Schaffner-Bielich, Phys. Rev. D **93**, 065011 (2016).
[32] R. Câmara Pereira, P. Costa, and C. Providência, Phys. Rev. D **94**, 094001 (2016).
[33] X. Wu, A. Ohnishi, and H. Shen, Phys. Rev. C **98**, 065801 (2018).
[34] I. F. Ranea-Sandoval, S. Han, M. G. Orsaria, G. A. Contrera, F. Weber, and M. G. Alford, Phys. Rev. C **93**, 045812 (2016).
[35] G. E. Brown and M. Rho, Phys. Rev. Lett. **66**, 2720 (1991).
[36] Y. Sugahara and H. Toki, Nucl. Phys. **A579**, 557 (1994).
[37] K. Sumiyoshi, H. Kuwabara, and H. Toki, Nucl. Phys. **A581**, 725 (1995).
[38] R. Casalbuoni, R. Gatto, G. Nardulli, and M. Ruggieri, Phys. Rev. D **68**, 034024 (2003).

[39] M. I. Gorenstein and S. N. Yang, Phys. Rev. D **52**, 5206 (1995).
[40] K. Schertler, C. Greiner, and M. Thoma, Nucl. Phys. **A616**, 659 (1997).
[41] D. Blaschke, A. Ayriyan, D. E. Alvarez-Castillo, and H. Grigorian, Universe **6**, 81 (2020).
[42] A. Drago, A. Lavagno, G. Pagliara, and D. Pigato, Phys. Rev. C **90**, 065809 (2014).
[43] P. Ribes, A. Ramos, L. Tolos, C. Gonzalez-Boquera, and M. Centelles, Astrophys. J. **883**, 168 (2019).
[44] J. J. Li and A. Sedrakian, Astrophys. J. **874**, L22 (2019).
[45] J. J. Li, A. Sedrakian, and M. Alford, Phys. Rev. D **101**, 063022 (2020).
[46] M. G. Alford, S. Han, and M. Prakash, Phys. Rev. D **88**, 083013 (2013).
[47] M. G. Alford and S. Han, Eur. Phys. J. A **52**, 62 (2016).
[48] S. Han, M. A. A. Mamun, S. Lalit, C. Constantinou, and M. Prakash, Phys. Rev. D **100**, 103022 (2019).
[49] E. Annala, T. Gorda, A. Kurkela, J. Nättilä, and A. Vuorinen, Nat. Phys. **16**, 907 (2020).
[50] I. Tews, J. Margueron, and S. Reddy, Phys. Rev. C **98**, 045804 (2018).
[51] J. Morais, B. Hiller, and A. A. Osipov, Phys. Rev. D **95**, 074033 (2017).
[52] K. Fukushima, Phys. Rev. D **77**, 114028 (2008); **78**, 039902 (E) (2008).
[53] R. Câmara Pereira, J. Moreira, and P. Costa, Eur. Phys. J. A **56**, 214 (2020).
[54] M. Ferreira, R. Câmara Pereira, and C. Providência, Phys. Rev. D **101**, 123030 (2020).
[55] K. A. Olive *et al.* (Particle Data Group), Chin. Phys. C **38**, 090001 (2014).
[56] G. A. Lalazissis, T. Nikšić, D. Vretenar, and P. Ring, Phys. Rev. C **71**, 024312 (2005).
[57] M. Dutra, O. Lourenço, S. Avancini, B. Carlson, A. Delfino, D. Menezes, C. Providência, S. Typel, and J. Stone, Phys. Rev. C **90**, 055203 (2014).
[58] M. Fortin, C. Providencia, A. Raduta, F. Gulminelli, J. L. Zdunik, P. Haensel, and M. Bejger, Phys. Rev. C **94**, 035804 (2016).
[59] K. Hebeler, J. Lattimer, C. Pethick, and A. Schwenk, Astrophys. J. **773**, 11 (2013).
[60] T. Klahn, D. Blaschke, F. Sandin, C. Fuchs, A. Faessler, H. Grigorian, G. Ropke, and J. Trumper, Phys. Lett. B **654**, 170 (2007).
[61] D. P. Menezes, M. B. Pinto, L. B. Castro, P. Costa, and C. Providência, Phys. Rev. C **89**, 055207 (2014).
[62] T. Klahn and T. Fischer, Astrophys. J. **810**, 134 (2015).
[63] M. G. Alford and S. Han, Eur. Phys. J. A **52**, 62 (2016).
[64] A. Kurkela, P. Romatschke, and A. Vuorinen, Phys. Rev. D **81**, 105021 (2010).
[65] R. C. Tolman, Phys. Rev. **55**, 364 (1939).
[66] J. R. Oppenheimer and G. M. Volkoff, Phys. Rev. **55**, 374 (1939).
[67] T. Hinderer, Astrophys. J. **677**, 1216 (2008).
[68] T. Hinderer, B. D. Lackey, R. N. Lang, and J. S. Read, Phys. Rev. D **81**, 123016 (2010).
[69] S. Postnikov, M. Prakash, and J. M. Lattimer, Phys. Rev. D **82**, 024016 (2010).
[70] M. Miller *et al.*, Astrophys. J. Lett. **887**, L24 (2019).
[71] B. P. Abbott *et al.* (Virgo and LIGO Scientific Collaborations), Phys. Rev. Lett. **121**, 161101 (2018).
[72] S. Weissenborn, D. Chatterjee, and J. Schaffner-Bielich, Nucl. Phys. **A914**, 421 (2013).
[73] M. Oertel, C. Providência, F. Gulminelli, and A. R. Raduta, J. Phys. G **42**, 075202 (2015).
[74] A. Bauswein, N.-U. F. Bastian, D. B. Blaschke, K. Chatziioannou, J. A. Clark, T. Fischer, and M. Oertel, Phys. Rev. Lett. **122**, 061102 (2019).